Journal of Pharmaceutical Analysis 2012;2(4):241–248

Contents lists available at ScienceDirect

Journal of Pharmaceutical Analysis

www.elsevier.com/locate/jpa
www.sciencedirect.com

ORIGINAL ARTICLE

Second-order calibration applied to quantification of two active components of *Schisandra chinensis* in complex matrix

Xiao-Hua Zhang, Hai-Long Wu*, Jian-Yao Wang, Yao Chen, Yong-Jie Yu, Chong-Chong Nie, Chao Kang, De-Zhu Tu, Ru-Qin Yu

State Key Laboratory of Chemo/Biosensing and Chemometrics, College of Chemistry and Chemical Engineering, Hunan University, Changsha 410082, PR China

Received 23 February 2012; accepted 9 April 2012
Available online 25 April 2012

KEYWORDS

Traditional Chinese medicine;
Second-order calibration;
Schizandrol A;
Schizandrin B;
Self-weighted alternating normalized residue fitting (SWANRF) algorithm;
Alternating normalization-weighted error (ANWE) algorithm.

Abstract The effectiveness of traditional Chinese medicine (TCM) against various diseases urges more low cost, speed and sensitive analytical methods for investigating the phamacology of TCM and providing a theoretical basis for clinical use. The potential of second-order calibration method was validated for the quantification of two effective ingredients of *Schisandra chinensis* in human plasma using spectrofluorimetry. The results obtained in the present study demonstrate the advantages of this strategy for multi-target determination in complex matrices. Although the spectra of the analytes are similar and a large number of interferences also exist, second-order calibration method could predict the accurate concentrations together with reasonable resolution of spectral profiles for analytes of interest owing to its 'second-order advantage'. Moreover, the method presented in this work allows one to simply experimental procedure as well as reduces the use of harmful chemical solvents.

1. Introduction

Traditional Chinese medicine (TCM) has attracted much attention due to their effectiveness against many diseases with relatively low toxicity, especially for treating various chronic diseases (for example, rheumatism and arthritis) [1,2]. Nowadays, the attention of researchers has been drawn towards various aspects of TCM, such as the pharmacological interpretation of their mechanisms of action, the scientific and clinical proof of their effectiveness, the quality control methods and the relative toxicity studies. These studies are inseparable from the analysis of the effective ingredients of TCM. At the same time, it is widely accepted that complex synergistic effects among vast number of chemical constituents

*Corresponding author. Tel.: +86 731 88821818; fax: +86 731 88821818.
E-mail address: hlwu@hnu.edu.cn (H.-L. Wu)

Peer review under responsibility of Xi'an Jiaotong University.
http://dx.doi.org/10.1016/j.jpha.2012.04.002

existing in TCM are responsible for the therapeutic effects [3,4].

Since then, the quantitative analysis of effective ingredients of TCM in complex matrices plays an important role in the studies of TCM. However, it poses great challenge to analysts owing both to the high complexity of the matrices and the low concentration levels of the analytes of interest. Numerous studies trying to analyze effective ingredients of TCM in complex matrices (e.g., medicinal herbs [5,6], herbal preparations [7,8], body fluids [9,10], etc) have been reported in recent years. The analysis is regularly achieved on high-performance liquid chromatography (HPLC) coupled with different detection systems [2,11–14]. As a powerful qualitative and quantitative analytical technique, HPLC possesses a number of advantages such as general applicability to a wide range of analytes and sensitivity due to the enhanced signal to noise ratio. However, due to the complexity of chemicals and the existence of unknown interferences in matrices, these measurement techniques are faced with many difficulties. They are almost time-consuming and demand tedious pretreatment procedures of extraction, pre-concentration and purification.

Among the benefits of fluorescence spectroscopy is the adaptability to field measurements, the high sensitivity to a wide array of potential analytes, and, in general, the avoidance of consumable reagents and extensive sample pretreatment [15]. Spectrofluorimetry could be a sensitive alternative for direct determination of effective ingredients of TCM, since they usually present natural fluorescence. However, the wide application of fluorescence techniques for complex matrices has been limited by the lack of selectivity of fluorescence spectroscopy. In multi-component mixtures the fluorescence signal is normally overlapped, and bad results will be obtained without tedious pretreatment procedures. In recent years, the combination of spectrofluorimetric data and second-order calibration method is a way to bridge the gap and has developed lots of applications for determining analytes in complex matrices. Examples of these second-order methods applied in spectrofluorimetric analysis are alternating trilinear decomposition algorithm (ATLD) [16], parallel factor analysis (PARAFAC) [17], self-weighted alternating trilinear decomposition algorithm (SWATLD) [18] and so on. They make quantitative possibility by mathematical removal of the signal contribution of interferences owing to their 'second-order advantage' [19,20], it allows one to simply experimental procedure, and save money as well as reduce the use of harmful chemical solvents.

S. chinensis, because of its various beneficial biological activities including hepatoprotective effect [21], potent antioxidative property [22], strong inhibiting effect on human immunodeficiency virus (HIV) [23,24], has been studied by researchers as an interesting and meaningful analyte. It is a famous medicinal plant native to East Asia. The modern pharmacological research has demonstrated that most of the biological activities and pharmacological effects of *S. chinensis* could be attributed to its didenzocyclooctadiene-type lignans represented by Schizandrol A (Sch A, Fig. 1(A)) and Schisandrin B (Sch B, Fig. 1(B)). Sch A and Sch B are the most abundant antioxidants, and main effective didenzocyclooctadiene derivatives isolated from the *S. chinensis*. The clinical efficacy of *S. chinensis* is related to its lignans concentrations in vivo which varies from patient to patient and has to be evaluated for each one. It is thus vital to quantify Sch A and Sch B in human plasma. Since the main fluorophores of Sch A and Sch B are both biphenyl group, their fluorescence excitation and emission spectra are very similar. Moreover, human plasma is composed of a variety of components and some of them make significant contributions to the overall fluorescence [25]. The spectra are overlapping severely between the analytes and tryptophan in plasma. Therefore, direct determination in human plasma is not feasible. We combine spectrofluorimetry with second-order calibration methods based on self-weighted alternating normalized residue fitting (SWANRF) algorithm and alternating normalization-weighted error (ANWE) algorithm to develop a direct method for simultaneous determining Sch A and Sch B in human plasma. The proposed method was validated through the estimation of figures of merit and statistic parameter. The results showed that the excitation and emission spectra of individual analytes were free from interference of sample matrix and the concentration values were estimated approvingly.

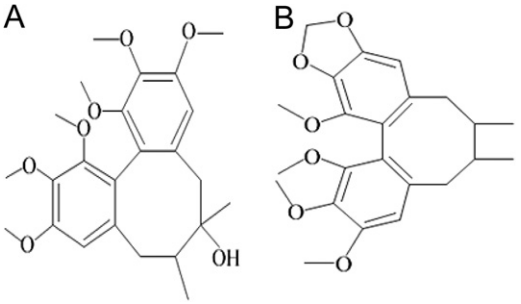

Figure 1 The chemical structure of Schizandrol A (A) and Schizandrin B (B).

2. Theory

2.1. Three-way trilinear data array

The outcome of each experimental measurement is a data matrix, having one excitation spectral mode and one emission spectral mode. Accordingly, when more samples are analyzed, the resulting data structure is a three-way data array. The trilinear model could be given by three profiling matrices, **A**, **B** and **C**, with elements a_{in}, b_{jn} and c_{kn}, respectively. The sum of squares of the residues, e_{ijk}, is minimized in the trilinear model, which is represented as follows:

$$x_{ijk} = \sum_{n=1}^{N} a_{in} b_{jn} c_{kn} + e_{ijk} \quad (i = 1, 2, \ldots, I; \quad j = 1, 2, \ldots, J; \quad k = 1, 2, \ldots, K)$$

2.2. Second-order calibration method

As can be seen from Fig. 2, second-order calibration could uniquely decompose the there-way data array stacked with a series of response matrices obtained from each sample. Based upon 'second-order advantage', the entire process consists of four steps in the present work.

First, the calibration set as well as the test set are designed. A series of two-way fluorescence response matrices are

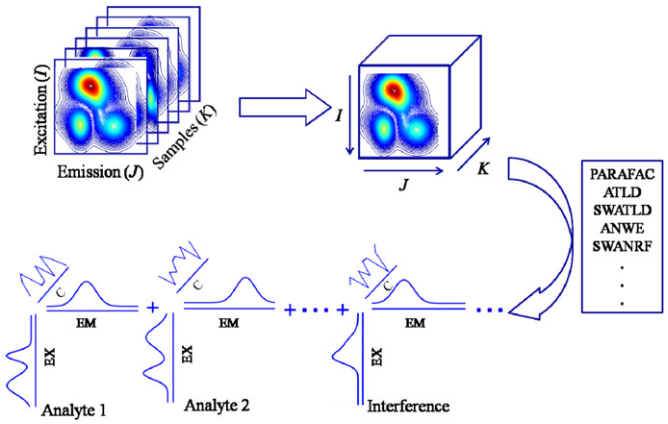

Figure 2 The graphical representation of second-order calibration method. EX: excitation spectrum; EM: emission spectrum; C: relative concentration profile.

acquired from each sample, and then stacked in one direction to form second-order fluorescence array. Second, the three-way data array is uniquely decomposed, and we can obtain the relative spectral matrices (**A**) and (**B**) and the relative concentrations (**C**) of individual components, even in the presence of unknown interferences. Third, the components are identified through the information including the relative excitation spectrum matrix **A** as well as the relative emission spectrum matrix **B**. Lastly, the concentration values in unknown samples are obtained by a regression of the relative concentration contributions of each component of interest versus its standard concentrations. The concrete steps of second-order calibration method can consult the literature [16].

In term of our experimental results, we selected SWANRF algorithm and ANWE algorithm which yielded satisfactory results. These two algorithms implement to three-way data could provide access to extract the spectral profiles reliably and estimate the concentrations of analytes of interest accurately even in the presence of unknown interferences. More details of the algorithms are described in the original literature [26,27].

3. Experimental

3.1. Reagents

Sch A (>98%) and Sch B (>98%) were purchased from Aladdin (Shanghai, China). Stock solutions of Sch A (152 μg/mL) and Sch B (106 μg/mL) were prepared in ethanol, since Sch A and Sch B have low solubility in water. They were stored in the brown volumetric flask at 4 °C. All the working solutions were prepared daily by appropriate dilution of the stock solutions with aqueous ethanol. Drug-free human plasma (frozen plasma) was kindly provided by the Blood Center in Changsha, and stored in a freezer at −20 °C. Ethanol and ethyl acetate was analytical grade and ultra pure water was prepared using a direct-pure plus water system (Rephile, China). All the glassware was previously soaked in chromate lotion overnight, and then cleaned with distilled water before use.

3.2. Apparatus and software

The fluorescent spectra were obtained in a Hitachi (Tokyo, Japan) F-7000 fluorescence spectrophotometer, using a 1 cm quartz cell. The run of the algorithms and the calculation were done using MATLAB R2009b. The SigmaPlot 10.0 software was used for data processing and graphical display.

3.3. Sample stability and linearity

The linear range is 0–8.68 μg/mL for Sch A. As for Sch B, the linear range is 0–10.2 μg/mL. The standard solutions of Sch A and Sch B were found stable for at least 15 day when stored at 4 °C.

3.4. Optimization of the solvent

The proportions (ethanol: ethanol water, v/v) including 10%–100% were studied to optimize the solvent. We measured the fluorescence spectra of Sch A in different solvents, since the fluorescence intensity of Sch A was lower than Sch B in the same concentration. The results (Fig. 3) indicate that the fluorescence intensity of Sch A increased first and then decreased along with the increase of the proportion of ethanol in the solvents, but the shape of the spectra is almost no change, the maximum fluorescence intensity is attained at 40% (ethanol: ethanol water, v/v). For one reason, the polarity of the solvent may influence the fluorescence intensity of the analytes. 40% ethanol water solution was used in the subsequent experiment as the preferred solvent.

3.5. Procedure

A preliminary treatment of plasma was carried out. 1 mL plasma was added in a tube respectively, and then mixed with 1 mL ethanol and 6 mL ethyl acetate. The mixtures were extracted by sonication for 15 min, followed by centrifugation at 10,000 rpm for 10 min at room temperature. The upper ethyl acetate layer was transferred to another tubes and dried at 40°C, then reconstituted with aqueous ethanol to 10 mL.

A seven-sample set was built for calibration with SWANRF and ANWE algorithms, respectively, where the concentration of Sch A is 0–5.32 μg/mL within its corresponding linear range, and

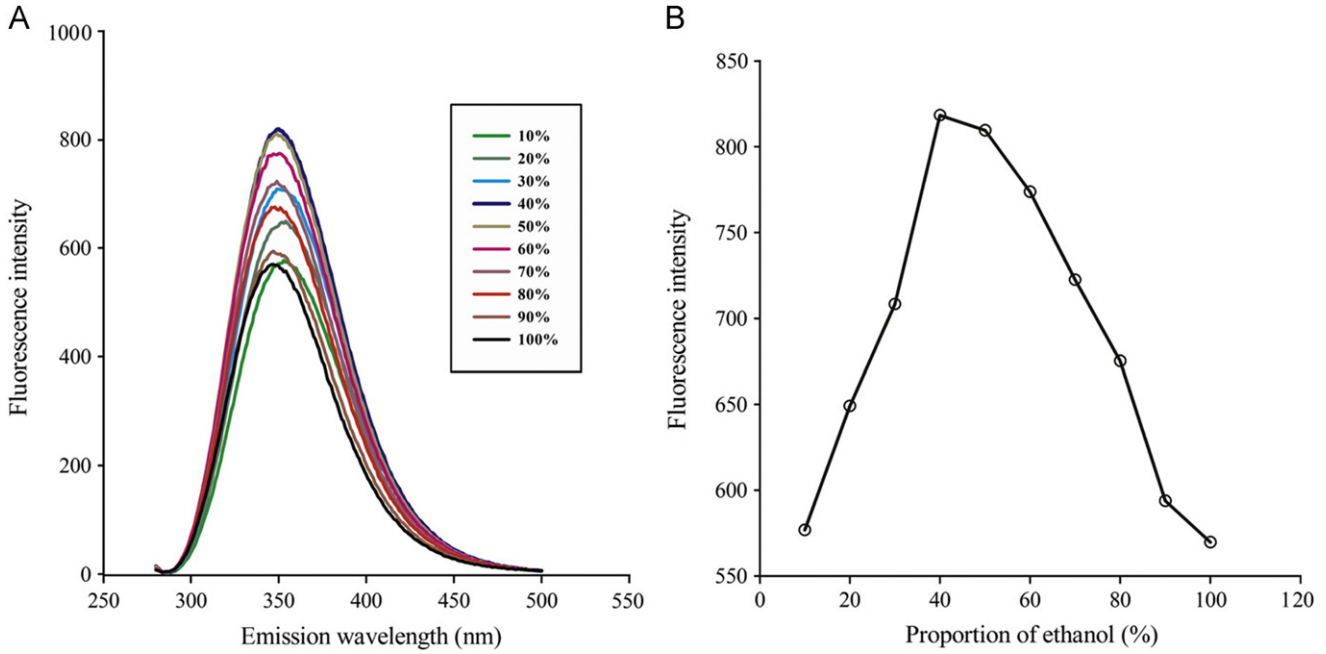

Figure 3 Emission spectrum (A) and fluorescence intensity (B) of Schizandrol A (197 μg/mL) in solvents with different proportions of ethanol and water.

Table 1 Schizandrol A and Schizandrin B concentrations in calibration set.

Sample	Sch A (μg/mL)	Sch B (μg/mL)
1	4.94	0.100
2	4.18	0.150
3	3.80	0.400
4	3.04	0.450
5	2.66	0.500
6	0.00	0.550
7	5.32	0.000

the concentration of Sch B is 0–0.550 μg/mL in the linear analytical range. On the other hand, a five-sample plasma set P1–P5 was created by adding 1mL the supernatant of plasma with different amount of Sch A and Sch B, then diluted to 10 mL with 40% aqueous ethanol in brown volumetric flasks. The final analyte concentrations are listed in Table 1 and 2.

All the three-way spectral surfaces were obtained in the excitation range from 200 to 330 nm (2 nm steps) and in the emission range from 280 to 500 nm (1 nm steps). The excitation and emission monochromator slit widths are 2.5/2.5 nm, and the scanning rate is 2400 nm/min. All the two-way emission spectra were obtained from 280 to 500 nm (1 nm steps), with fixed excitation wavelength of 257 nm. The slit width is 2.5/2.5 nm, and the scanning rate is 60 nm/min.

3.6. *Data pretreatment*

In this work, to avoid the effect of Rayleigh and Raman scattering signals which don't contain any available information, the response matrices were simply disposed just by truncating the data account for the Rayleigh-scattering signal, and subtracting the average response matrix of three drug-free blank solutions. Therefore, the size of optimum excitation–emission fluorescence matrices is 30×164 (excitation wavelengths $\times$ emission wavelengths).

4. Results and discussion

4.1. *Fluorescent spectra for Sch A and Sch B*

Fig. 4 displays spectral surfaces of the pure Sch A sample and Sch B sample, the plasma sample as well as the plasma-based sample (i.e., including Sch A, Sch B and plasma interference). Sch A, near the center of the images, has an excitation maximum near to 255 nm and emission maximum around 347 nm. The spectra of Sch B are similar to Sch A, it has maxima at approximately 257 nm excitation and 351 nm emission and fluorescence more stronger than the intensity of Sch A at the same concentration. As for the EEM spectra of plasma-based sample, the sum of the fluorescence intensity is equal to the intensity of plasma background and the analytes, so the observed spectrum is more complicated and the intensity increases. The approximate structures of the two analytes result in the slight difference in the spectral domains, their fluorescence excitation and emission spectra overlap severely, as can be seen in Fig. 5. On the other hand, highly overlapping profiles actually occur among analytes of interest and the interferences in plasma matrix.

Consequently, traditional spectrofluorimetric methods are not feasible to simultaneous determine Sch A and Sch B in plasma samples without previous separation procedures. Our option to solve this challenge is to employ second-order

Table 2 Analytical results for Schizandrol A and Schizandrin B.

Sample	Added concentration (μg/mL)		Predicted concentration (μg/mL)			
	Sch A	Sch B	Sch A		Sch B	
			SWANRF	ANWE	SWANRF	ANWE
P1	3.72	0.230	3.28 (88.3)[a]	3.56 (95.8)	0.214 (93.0)	0.210 (91.1)
P2	3.34	0.240	3.13 (93.7)	3.28 (98.3)	0.232 (96.6)	0.238 (99.1)
P3	2.96	0.280	2.66 (90.0)	2.76 (93.3)	0.255 (91.1)	0.267 (95.5)
P4	2.85	0.380	2.47 (86.8)	2.66 (93.3)	0.324 (85.2)	0.327 (86.0)
P5	2.47	0.390	2.28 (92.5)	2.30 (93.2)	0.350 (89.6)	0.368 (94.4)
Average recovery (%)			90.3±2.3	94.8±1.8	91.1±3.0	93.2±3.7

[a]Recovery in parenthesis.

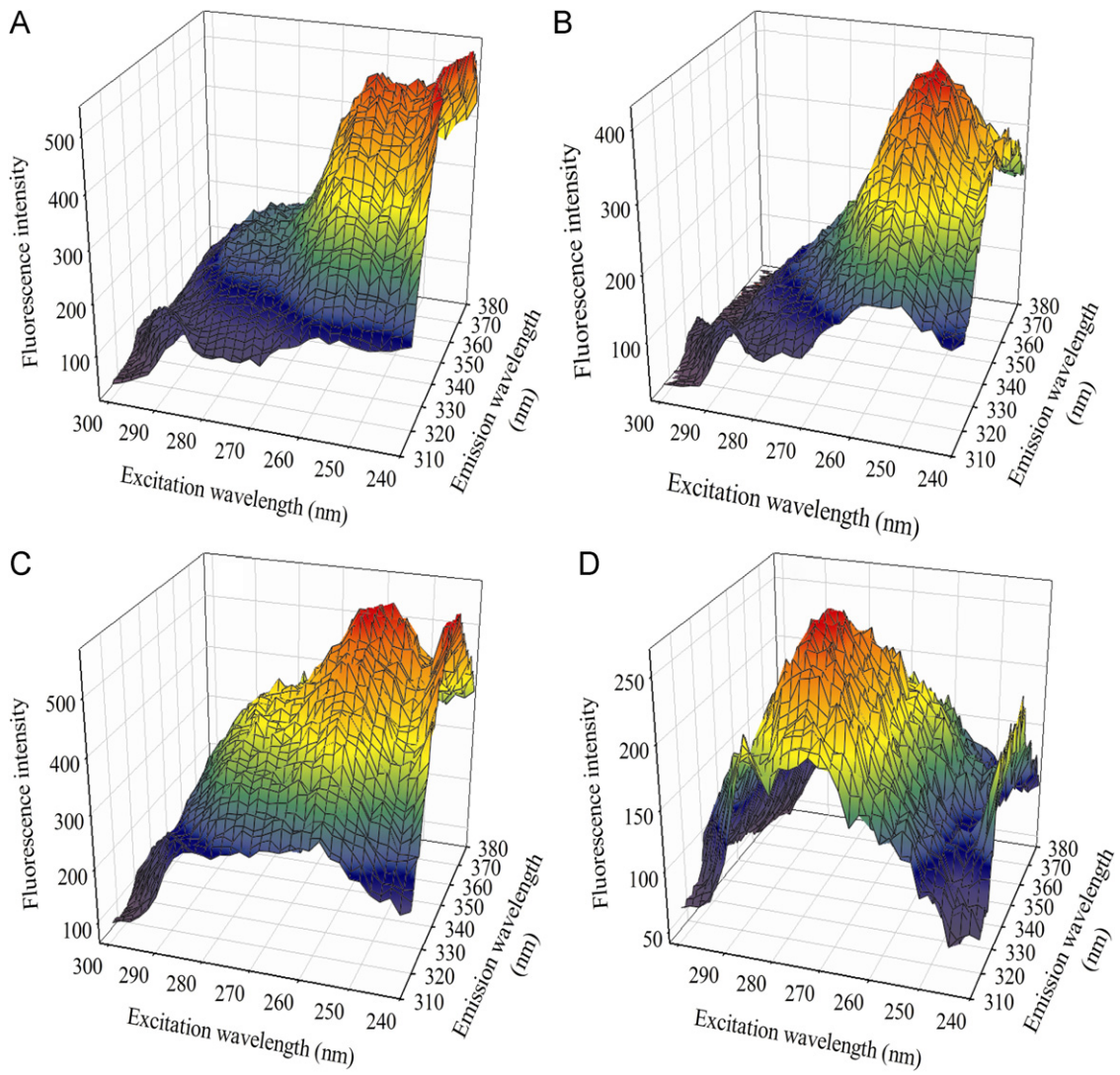

Figure 4 Three-dimensional plots of the excitation–emission matrix fluorescence spectra of (A) Schizandrol A (5.32 μg/mL), (B) Schizandrin B (0.550 μg/mL), (C) plasma-based sample P5 and (D) plasma (diluted 100 times).

calibration methods based on SWANRF and ANWE algorithms to resolve each of the analyte profiles from any uncalibrated spectroscopic interferences (i.e., fluorescent background, other fluorescent analytes, or Raman scattering) on of the well-established 'second-order advantage'.

4.2. Simultaneous determination of Schizandrol A and Schizandrin B in plasma samples

SWANRF and ANWE algorithms were used to quantitative determination of Sch A and Sch B in plasma matrix in this

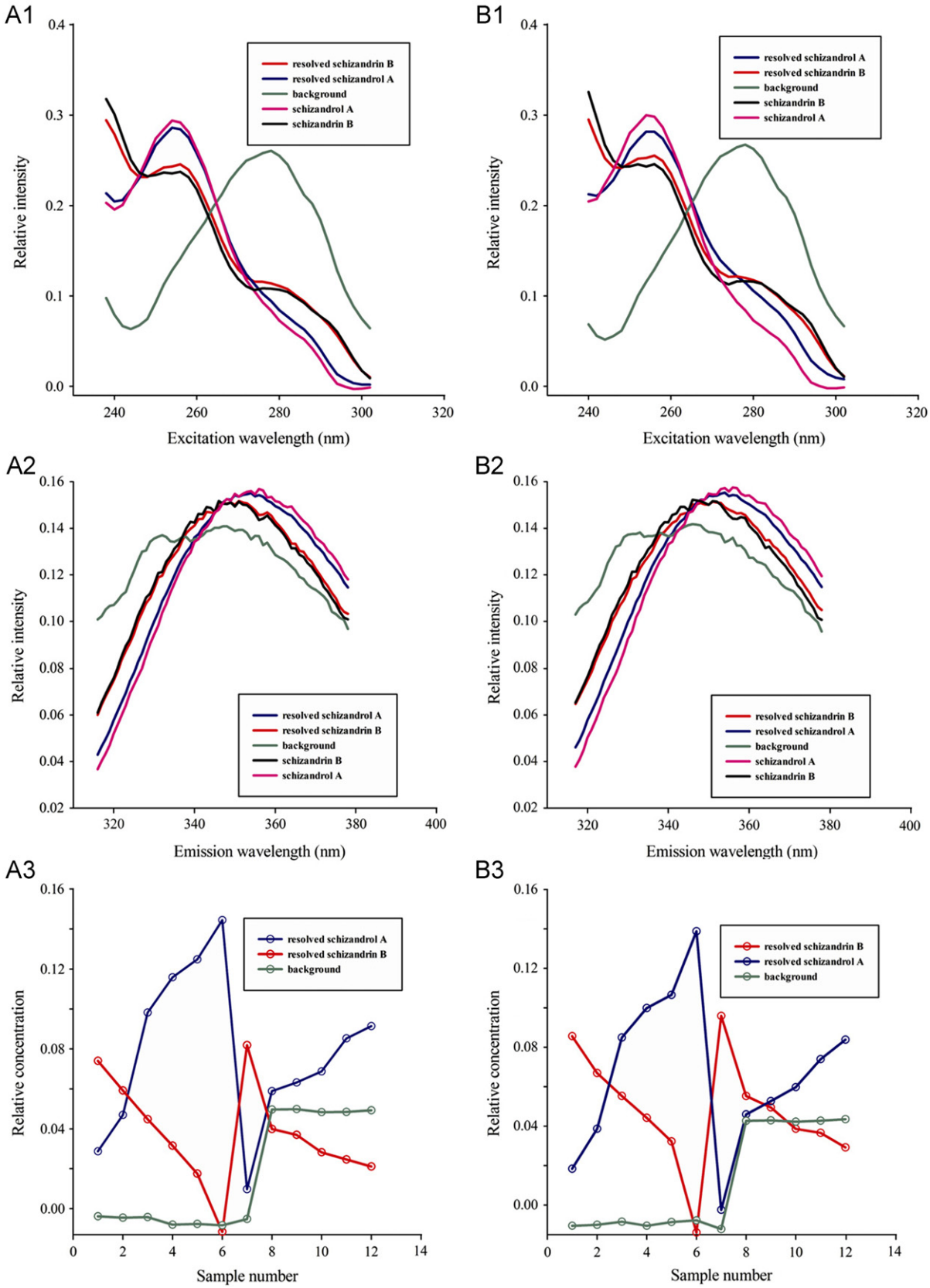

Figure 5 The resolved spectra of Schizandrol A and Schizandrin B from SWANRF (A1, A2, A3) and ANWE (B1, B2, B3) and the actual spectral profiles.

Table 3 Statistical validation results for Schizandrol A and Schizandrin B.

Parameter	Sch A		Sch B	
	SWANRF	ANWE	SWANRF	ANWE
SEN$*10^3$ (mL/μg)	0.178	0.190	3.41	3.46
SEL	0.0942	0.0903	0.142	0.145
LOD (ng/mL)[a]	165	199	3.20	2.90
RMSEP (ng/mL)[b]	908	825	112	99

[a]LOD = 3.3 s(0), LOQ = 10 s(0), where s(0) is the standard deviation in the predicted concentrations of the target analytes for three different background blank samples.

[b]$\mathrm{RMSEP} = \sqrt{1/n\text{-}1 \sum_{l=1}^{n} (d_l\text{-}\hat{d}_l)^2}$ where d_l and $\hat{d}_l$ are the actual and predicted concentrations of the analytes, respectively.

work. Since these two algorithms are insensitive to the component number, they can perform well with more acceptable calibration and resolution and give good results, so long as the factors are equal to or greater than the actual ones. In the excitation and emission region of the analytes, the fluorescence of plasma is basically due the strong fluorescence of tryptophan. Therefore, three factors including two target analytes and one natural interference from the plasma matrix were the best choice in this work.

The three-way data array was decomposed to obtain two spectral matrices (**A**) and (**B**) related to the excitation mode and emission mode, respectively, as well as a concentration matrix (**C**) composed of the relative concentrations of individual components in the samples. The estimated spectra were depicted in Fig. 5. High similarity between the resolved elution profiles and those of the solution standards confirmed the accuracy and reliability of the proposed strategy, which fully exploited 'second-order advantage' irrespective to the complexity of the matrix studied. The predicted results for Sch A and Sch B based on the SWANRF and ANWE algorithms are summarized in Table 2 (as the percentage ratio between the predicted and the true concentrations). The results should be considered to be well considering the complexity of the background and the heavily overlapped peaks between analytes. The recoveries obtained by using both SWANRF and ANWE algorithms are similar (>90%), highlighting that the second-order calibration methods based on these two algorithms are capable of reliably quantifying Sch A and Sch B in complex plasma samples.

4.3. *Method validation*

To evaluate the performance of the developed method, the validation parameters including sensitivity (SEN), selectivity (SEL), root-mean-square error of prediction (RMSEP), and limit of detection (LOD) have been calculated. The SEN value and SEL value are estimated by the following Eqs. [28]:

$$\mathrm{SEN} = k\{[(\mathbf{A}_{exp}^{T}\mathbf{P}_{a,unx}\mathbf{A}_{exp})*(\mathbf{B}_{exp}^{T}\mathbf{P}_{b,unx}\mathbf{B}_{exp})]^{-1}\}_{nn}^{-1/2}$$

$$\mathrm{SEL} = \{[(\mathbf{A}_{exp}^{T}\mathbf{P}_{a,unx}\mathbf{A}_{exp})*(\mathbf{B}_{exp}^{T}\mathbf{P}_{b,unx}\mathbf{B}_{exp})]^{-1}\}_{nn}^{-1/2}$$

where $\mathbf{P}_{a,unx} = \mathbf{I} - \mathbf{A}_{unx}\mathbf{A}_{unx}^{+}$, $\mathbf{P}_{b,unx} = \mathbf{I} - \mathbf{B}_{unx}\mathbf{B}_{unx}^{+}$, $\mathbf{A}_{\mathrm{unx}}$ and $\mathbf{B}_{\mathrm{unx}}$ contain the profiles for the unexpected components as columns, $\mathbf{A}_{exp}$ and $\mathbf{B}_{exp}$ are the matrices containing the profiles for all expected components in each dimension, k is the integrated total signal for component n at unit concentration.

Table 3 summarizes the validation parameters for the method based on SWANRF and ANWE algorithms. It seems that the validation parameters of Sch B are better than Sch A, and the values of both substances are satisfactory. The LOD values and RMSEP values of Sch B are lower than Sch A, the SEN values and SEL values for Sch B are much larger than Sch A. The most important issue is that the fluorescence intensity of Sch B is higher than Sch A at the same concentration. The LOD values obtained by the two algorithms are almost the same and approximately 180 ng/mL for Sch A and 3.00 ng/mL for Sch B, and the corresponding plasma concentrations are 18.0 and 0.300 μg/mL. Obviously, the values got in this study for Sch B are far lower than the mean plasma concentration after i.g compound wurenchun capsules to rats, and the values for Sch A are in agreement with the report [29].

5. Conclusions

This study showed that second-order calibration method is a powerful chemometric tool for resolving heavily overlapped peaks into their pure excitation, emission profiles and concentration information even in complicated matrices. Nowadays, traditional Chinese medicine (TCM) analysis has attracted much attention due to their important role against various diseases. Unfortunately, the traditional methods need a long time and it cannot obtain good results without tedious pretreatment procedures. Alternatively, the combination of spectrofluorimetry and second-order calibration method can simultaneous determine the effective ingredients of TCM in complex matrices. Second-order calibration method could predict the accurate concentrations together with reasonable resolution of excitation and emission profiles for the analytes of interest from any uncalibrated spectroscopic interferences on account of 'second-order advantage'. The results presented in this paper indicate that the combining spectrofluorimetry with second-order calibration method is good approaches for the fast direct analysis of effective ingredients of TCM in complicated systems.

Acknowledgments

The authors gratefully acknowledge the National Natural Science Foundation of China (Grant No. 21175041), the National Basic Research Program (Grant No. 2012CB910602) and Program for Changjiang Scholars and Innovative Research Team in University (PCSIRT) for financial supports.

References

[1] X.X. Yang, X.X. Zhang, R.M. Chang, et al., Simultaneous quantification of five major active components in capsules of the traditional Chinese medicine 'Shu-Jin-Zhi-Tong' by high performance liquid chromatography, J. Pharm. Anal. 1 (4) (2011) 284–290.

[2] Y.H. Wang, C. Qiu, D.W. Wang, et al., Identification of multiple constituents in the traditional Chinese medicine formula Sheng-Mai

San and rat plasma after oral administration by HPLC-DAD-MS/MS, J. Pharm. Biomed. Anal. 54 (5) (2011) 1110–1127.
[3] D. Normile, The new face of traditional Chinese medicine, Science 299 (5604) (2003) 188–190.
[4] W.Y. Jiang, Therapeutic wisdom in traditional Chinese medicine: a perspective from modern science, Trends Pharmacol. Sci. 26 (11) (2005) 558–563.
[5] G. Yuan, Y. Liu, T. Li, et al., Simultaneous and rapid determination of main lignans in different parts of schisandra sphenanthera by micellar electrokinetic capillary chromatography, Molecules 16 (5) (2011) 3713–3722.
[6] X.F. Chen, H.T. Wu, G.G. Tan, et al., Liquid chromatography coupled with time-of-flight and ion trap mass spectrometry for qualitative analysis of herbal medicines, J. Pharmacol. Anal. 1 (4) (2011) 235–245.
[7] G. Cao, C. Zhang, Y. Zhang, et al., Global detection and identification of components from crude and processed traditional Chinese medicine by liquid chromatography connected with hybrid ion trap and time-of-flight–mass spectrometry, J. Sep. Sci. 34 (15) (2011) 1845–1852.
[8] H. Huang, L. Ji, S. Song, et al., Identification of the major constituents in Xuebijing injection by HPLC-ESI-MS, Phytochem. Anal. 22 (4) (2011) 330–338.
[9] J. Yang, S.P. Ip, H.J Yeung, et al., HPLC-MS analysis of Schisandra lignans and their metabolites in Caco-2 cell monolayer and rat everted gut sac models and in rat plasma, Acta Pharm. Sin. B 1 (1) (2011) 46–55.
[10] X. Wang, H. Sun, A. Zhang, et al., Pharmacokinetics screening for multi-components absorbed in the rat plasma after oral administration traditional Chinese medicine formula Yin-Chen-Hao-Tang by ultra performance liquid chromatography-electrospray ionization/quadrupole-time-of-flight mass spectrometry combined with pattern recognition methods, Analyst 136 (23) (2011) 5068–5076.
[11] H.J. Lee, C.Y. Kim, Simultaneous determination of nine lignans using pressurized liquid extraction and HPLC-DAD in the fruits of *Schisandra chinensis*, Food Chem. 120 (4) (2010) 1224–1228.
[12] H. Zhang, G. Zhang, Z. Zhu, et al., Determination of six lignans in *Schisandra chinensis* (Turcz.) Baill Fruits and related Chinese multiherb remedies by HPLC, Food Chem. 115 (2) (2009) 735–739.
[13] B.L. Wang, J.P. Hu, W. Tan, et al., Simultaneous quantification of four active schisandra lignans from a traditional Chinese medicine *Schisandra chinensis* (Wuweizi) in rat plasma using liquid chromatography/mass spectrometry, J. Chromatogr. B 865 (1-2) (2008) 114–120.
[14] S. Mao, H. Zhang, L. Lv, et al., Rapid determination and pharmacokinetics study of lignans in rat plasma after oral administration of *Schisandra chinensis* extract and pure deoxyschisandrin, Biomed. Chromatogr. 25 (7) (2010) 808–815.
[15] R.D. Jiji, G.A. Cooper, K.S. Booksh, Excitation–emission matrix fluorescence based determination of carbamate pesticides and polycyclic aromatic hydrocarbons, Anal. Chim. Acta 397 (1–3) (1999) 61–72.
[16] H.L. Wu, M. Shibukawa, K. Oguma, An alternating trilinear decomposition algorithm with application to calibration of HPLC-DAD for simultaneous determination of overlapped chlorinated aromatic hydrocarbons, J. Chemom. 12 (1) (1998) 1–26.
[17] R. Bro, PARAFAC. Tutorial and applications, Chemom. Intell. Lab. Syst. 38 (2) (1997) 149–171.
[18] Z.P. Chen, H.L. Wu, J.H. Jiang, et al., A novel trilinear decomposition algorithm for second-order linear calibration, Chemom. Intell. Lab. Syst. 52 (1) (2000) 75–86.
[19] E. Sanchez, B.R. Kowalski, Tensorial resolution: a direct trilinear decomposition, J. Chemom. 4 (1) (1990) 29–45.
[20] E. Sanchez, B.R. Kowalski, Generalized rank annihilation factor analysis, Anal. Chem. 58 (2) (1986) 496–499.
[21] K.T. Liu, T. Cresteil, S. Columelli, et al., Pharmacological properties of dibenzo [a, c] cyclooctene derivatives isolated from Fructus Schizandrae chinensis II. Induction of phenobarbital-like hepatic monooxygen ases, Chem. Biol. Interact. 39 (3) (1982) 315–330.
[22] K.M. Ko, B.Y.H. Lam, Schisandrin B protects against *tert*-butylhydroperoxide induced cerebral toxicity by enhancing glutathione antioxidant status in mouse brain, Mol. Cell. Biochem. 238 (1) (2002) 181–186.
[23] G.Y. Yang, Y.K. Li, R.R. Wang, et al., Dibenzocyclooctadiene lignans from *Schisandra wilsoniana* and their anti-HIV-1 activities, J. Nat. Prod. 73 (5) (2010) 915–919.
[24] W.L. Xiao, R.R. Wang, W. Zhao, et al., Anti-HIV-1 activity of lignans from the fruits of *Schisandra rubriflora*, Arch. Pharm. Res. 33 (5) (2010) 697–701.
[25] O.S. Wolfbeis, M. Leiner, Mapping of the total fluorescence of human blood serum as a new method for its characterization, Anal. Chim. Acta 167 (1) (1985) 203–215.
[26] J.F. Nie, H.L. Wu, S.R. Zhang, et al., Self-weighted alternating normalized residue fitting algorithm with application to quantitative analysis of excitation–emission matrix fluorescence data, Anal. Methods 1 (2) (2010) 1918–1926.
[27] A.L. Xia, H.L. Wu, S.H. Zhu, et al., Determination of psoralen in human plasma using excitation–emission matrix fluorescence coupled to second-order calibration, Anal. Sci. 24 (9) (2008) 1171–1176.
[28] A.C. Olivieri, N.K.M. Faber, A closed-form expression for computing the sensitivity in second-order bilinear calibration, J. Chemom. 19 (11–12) (2005) 583–592.
[29] L. Luo, Z.H. Dou, A.W. Ding, et al., Comparison of schisandrin and schisandrin B in rat serum and plasma after ig compound wurenchun capsules, Chin. Tradit. Herb. Drugs 37 (10) (2006) 1486–1489.